

18

19 **Figure. S1. The secreted RAB22A-NeoF1 fusion protein enhances**
20 **metastasis in osteosarcoma.**

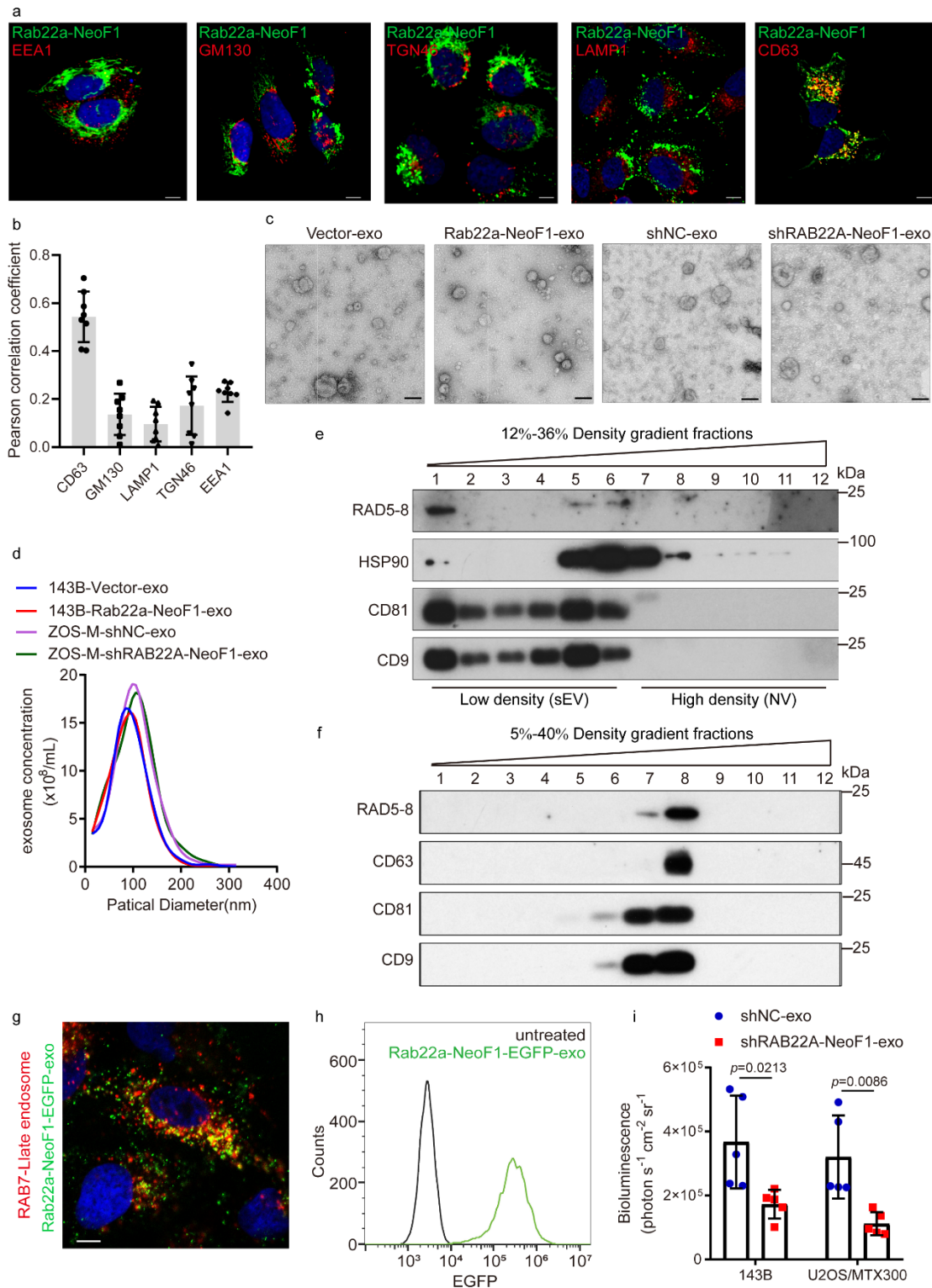
21 **(a)** Bioluminescence analyses of lung metastases from mice orthotopically
22 injected with the indicated cells under treatment of either Vector-CM or
23 RAB22A-NeoF1 CM. $n = 5$ biologically independent mice. Data are mean \pm s.d.
24 P values are shown.

25 **(b)** 143B cells were co-cultured with the indicated stable cells for 5 days and
26 then were subjected to migration and invasion assays. Data are mean \pm s.d. of
27 $n = 3$ biologically independent experiments. P values are shown.

28 **(c-f)** Representative IVIS imaging **(c)**, Bioluminescence analyses **(d)**

29 H&E-stained lung sections (**e**) and quantification of lung metastatic foci (**f**) from
30 mice orthotopically co-injected 143B-Luc cells with either ZOS-M-shNC cells or
31 ZOS-M-shRAB22A-NeoF1 cells at the 1:1 ratio. n = 5 biologically independent
32 mice. Data are mean \pm s.d. *P* values are shown. Scale bar, 2mm.

33 (**g**) Bioluminescence analyses of lung metastases from mice orthotopically
34 injected U2OS/MTX300-Luc cells alone or with either ZOS-M-shNC cells or
35 ZOS-M-shRAB22A-NeoF1 cells at the indicated 10:1 and 10:2 ratios. n = 5
36 biologically independent mice. Data are mean \pm s.d. *P* values are shown.



37

38 **Figure. S2. The RAB22A-NeoF1 fusion protein is present in exosomes to**
 39 **promote osteosarcoma metastasis.**

40 (a) Representative images of immunofluorescence staining for both
 41 intracellular RAB22A-NeoF1 and the indicated subcellular markers in U2OS
 42 cells stably expressing RAB22A-NeoF1. Scale bar, 5 μm.

43 **(b)** Pearson correlation coefficients (PCCs) were calculated from multiple
44 individual cells expressing RAB22A-NeoF1 and the indicated subcellular
45 markers. mean \pm SD. n = 8 fields. Data are mean \pm s.d.

46 **(c)** Characterization of exosomes derived from the indicated stable 143B cells
47 and stable ZOS-M cells using nanoparticle tracking analysis.

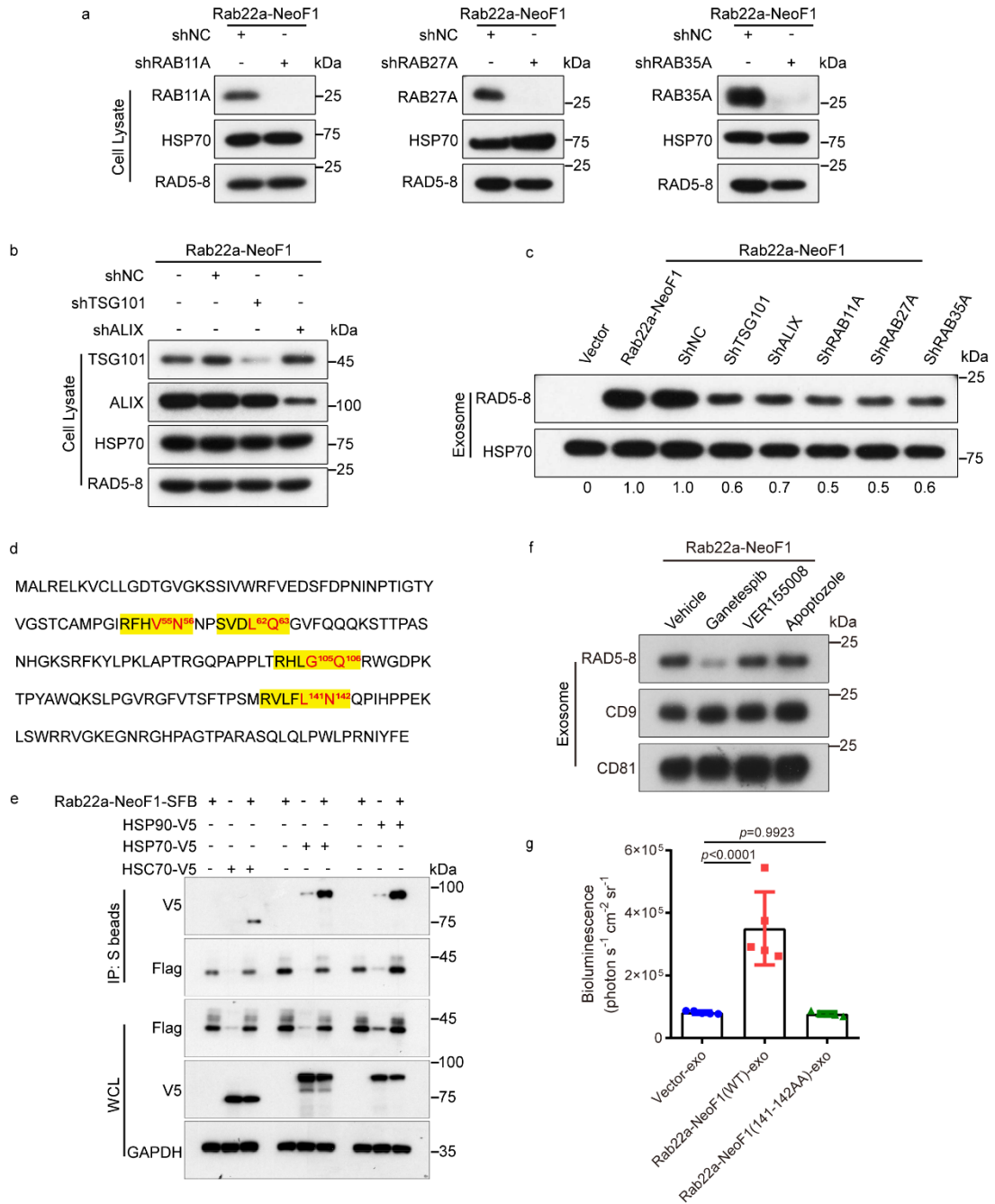
48 **(d)** Representative TEM images of the purified exosomes derived from the
49 indicated stable 143B (up two panels) and stable ZOS-M cells (low two panels).
50 Scale bar, 100nm.

51 **(e, f)** 12-36% **(e)** and 5%-40% **(f)** iodixanol density gradients centrifugation
52 was performed using the exosomes derived from 143B cells stably expressing
53 RAB22A-NeoF1 as described in "Materials and Methods" and followed by
54 Western blotting. Data in e and f are representative of n = 3 biologically
55 independent experiments.

56 **(g)** Representative confocal microscopy image of U2OS cells treated with
57 exosomes derived from 143B cells stably expressing Rab22a-NeoF1-EGFP
58 (Rab22a-NeoF1-EGFP-exo) for 15min. The late endosomes (Red, denoted by
59 RAB7) and GFP signals (Green) were shown. Scale bar, 5 μ m.

60 **(h)** The U2OS cells were treated with or without exosomes derived from 143B
61 cells stably expressing Rab22a-NeoF1-GFP (Rab22a-NeoF1-EGFP-exo) for
62 15 min, and subjected to flow cytometry analysis.

63 **(i)** Bioluminescence analyses of lung metastases from mice orthotopically
64 injected with the indicated cells under treatment of exosomes derived from the
65 indicated stable ZOS-M cells. n = 5 biologically independent mice. Data are
66 mean \pm s.d. *P* values are shown.



67

68 **Figure. S3. RAB22A-NeoF1 fusion protein is sorted into exosomes via**
 69 **binding to HSP90 to promote osteosarcoma metastasis**

70 (a, b) The indicated stable 143B cells were lysed and analyzed by Western
 71 blotting.

72 (c) The exosomes from the indicated stable 143B cells were purified and
 73 analyzed by Western blotting. The relative intensity of RAB22A-NeoF1 was
 74 quantified with ImageJ software and normalized with HSP70. Data in a-c are
 75 representative of n = 3 biologically independent experiments.

76

77 **(d)** The protein sequence of RAB22A-NeoF1. The yellow region indicates four
78 KFERQ-like motifs (aa52-56, aa59-63, aa102-106 and aa137-142) and
79 mutated amino acids are highlighted in red.

80 **(e)** 293T cells were co-transfected with the indicated plasmids and then were
81 lysed and analyzed by immunoprecipitation using S protein beads and
82 Western blotting.

83 **(f)** The 143B cells stably expressing Rab22a-NeoF1 were treated with the
84 HSP90 inhibitor (Ganetespib), HSP70 and HSC70 inhibitors (VER155008 and
85 Apoptozole) for 24h, and then the exosomes were purified and analyzed by
86 Western blotting. Data in e and f are representative of n = 3 biologically
87 independent experiments.

88 **(g)** Bioluminescence analysis of lung metastasis from mice orthotopically
89 injected 143B-Luc cells with exosomes derived from the indicated stable 143B
90 cells. n = 5 biologically independent mice. Data are mean \pm s.d. *P* values are
91 shown.

99 Proteins with significant increase from exosomes positive for RAB22A-NeoF1
100 were marked in red.

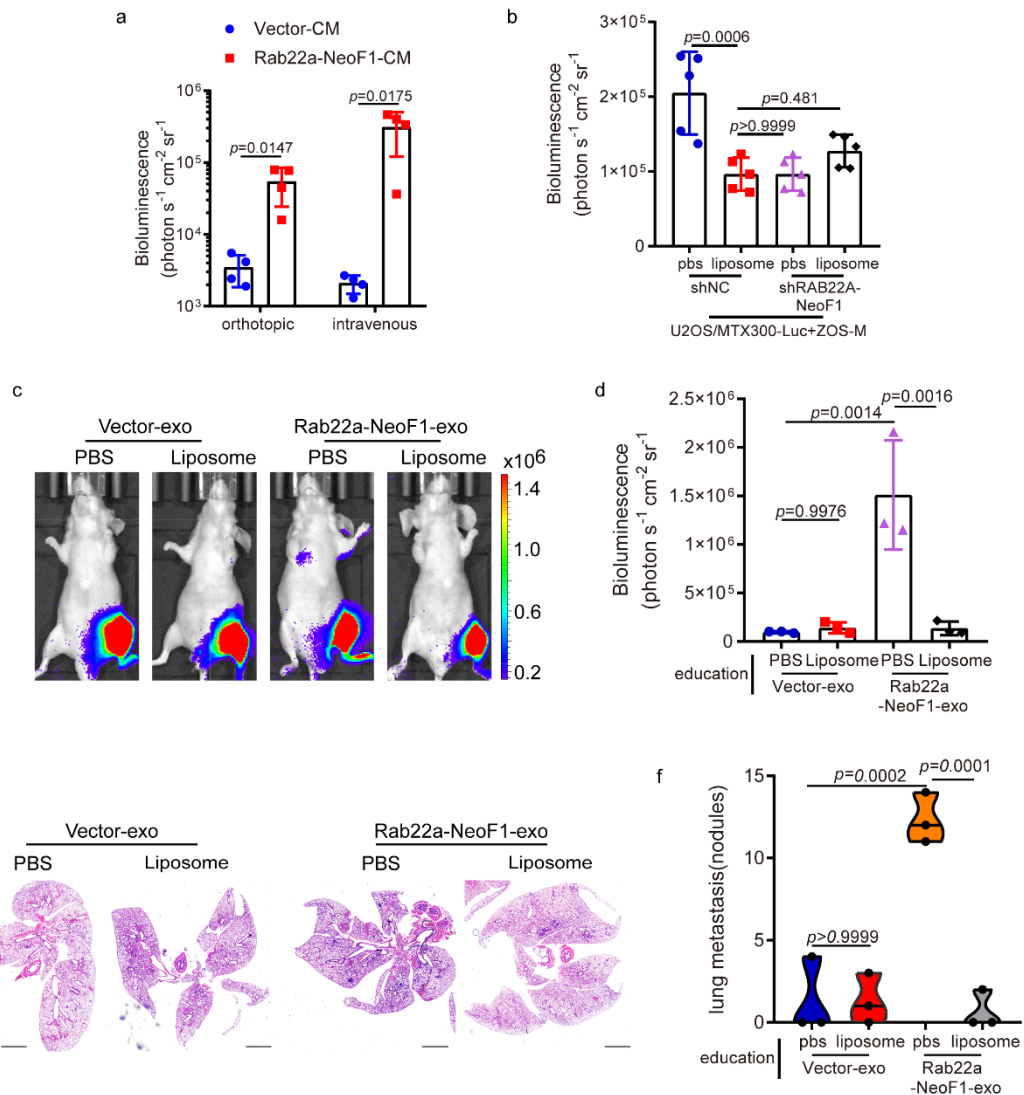
101 **(c)** 293T cells were co-transfected with the indicated plasmids and then were
102 lysed and analyzed by immunoprecipitation using anti-Flag beads or anti-V5
103 beads and Western blotting.

104 **(d)** 143B cells treated with exosomes derived from the indicated stable 143B
105 cells for 1 h, and then were subjected to the RhoA activation assay. The
106 relative intensity of RhoA-GTP quantified with ImageJ software and normalized
107 with RhoA-Total. Data in c and d are representative of $n = 3$ biologically
108 independent experiments.

109 **(e)** U2OS and 143B cells were treated with or without RhoA inhibitor CT04 for
110 4h, and then were incubated with exosomes derived from the indicated stable
111 143B cells for 24h. The cells were then collected and subjected to migration
112 and invasion assays. Data are mean \pm s.d. of $n = 3$ biologically independent
113 experiments. *P* values are shown.

114 **(f)** The exosomes and cell lysates were prepared from the indicated stable
115 143B cells, and then were analyzed by Western blotting. Data are
116 representative of $n = 3$ biologically independent experiments.

117 **(g)** Bioluminescence analysis of lung metastatic foci from mice orthotopically
118 injected 143B-Luc cells, and then were treated with the indicated exosomes.
119 $n = 5$ biologically independent mice. Data are mean \pm s.d. *P* values are shown.



120

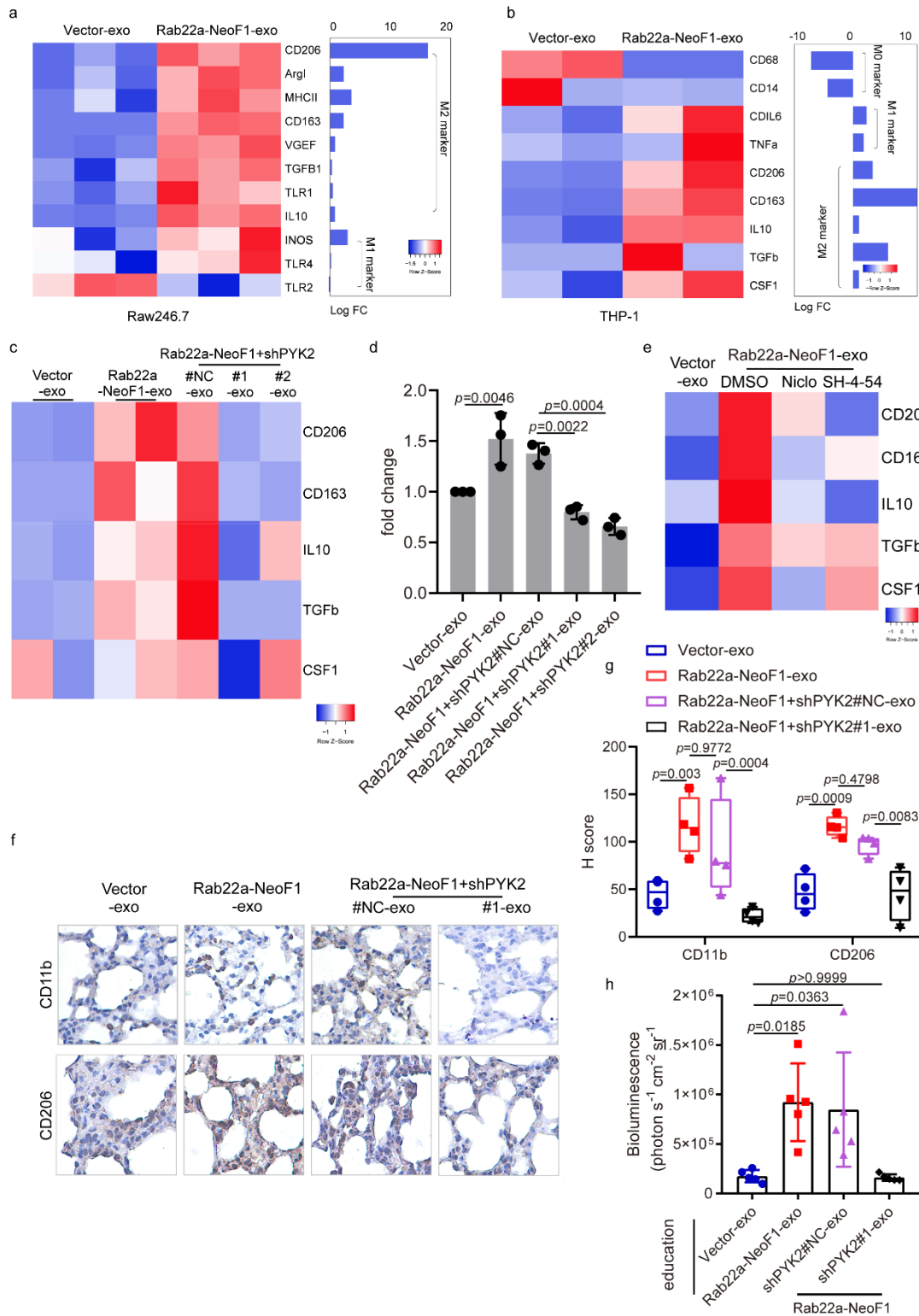
121 **Figure. S5. The functions of exosomal RAB22A-NeoF1 fusion protein**
 122 **requires recruiting BMDMs to pulmonary pre-metastatic niche.**

123 (a) Mice were pre-educated with the indicated conditioned media (CM) for 3
 124 weeks, and then were orthotopically or tail vein injected with 143B-Luc cells.
 125 The lung metastases were analyzed by Bioluminescence after 3 weeks. n =4
 126 biologically independent mice. Data are mean ± s.d. *P* values are shown.

127 (b) Mice orthotopically co-injected U2OS/MTX300-Luc cells with the indicated
 128 stable ZOS-M cells at the 10:1 ratio, and then intravenously injected liposome
 129 or PBS twice a week. The lung metastases were analyzed by bioluminescence.
 130 n = 5 biologically independent mice. Data are mean ± s.d. *P* values are shown.

131 (c-f) Mice were pre-educated with the indicated exosomes combined with
 132 liposome or PBS for 3 weeks, and then were orthotopically injected with

133 143B-Luc cells. The lung metastases were analyzed after 3 weeks.
134 Representative IVIS imaging (c), Bioluminescence analysis (d), H&E-stained
135 lung sections (e), Quantification of lung metastatic foci (f). n = 3 biologically
136 independent mice. Data are mean \pm s.d. *P* values are shown. Scale bar, 2mm.



137

138

Figure. S6. The exosomal RAB22A-NeoF1 fusion protein promotes M2 polarization in its recipient macrophages via its binding partner PYK2.

139

140

(a, b) Raw264.7 cells **(a)** and THP-1 cells **(b)** were incubated with the indicated

141

exosomes for 24 h, and differential expression patterns of the M0, M1 and M2

142

phenotype markers were presented by a heatmap.

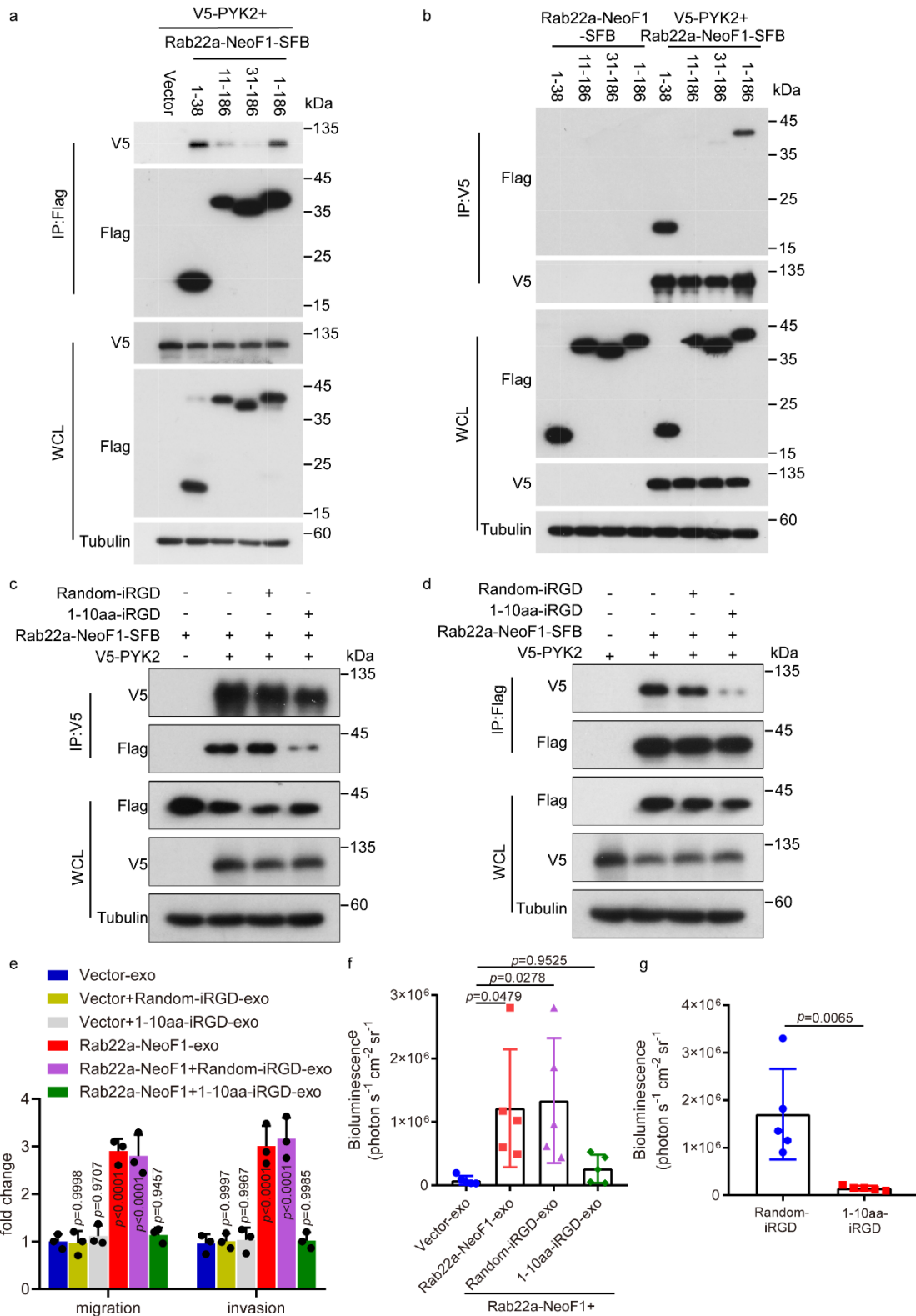
143 (c) THP-1 cells were incubated with the indicated exosomes for 24 h, and
144 differential expression patterns of the M2 polarization macrophage markers
145 were presented by a heatmap.

146 (d) Raw264.7 cells were incubated with the indicated exosomes for 24h, and
147 were subjected to migration assays. Data are mean \pm s.d. of n = 3 biologically
148 independent experiments. *P* values are shown.

149 (e) Raw264.7 cells were treated the indicated exosomes with or without the
150 indicated Stat3 inhibitor, Niclosamide or SH-4-54, for 24h and expression of
151 M2-like macrophage markers were present by a heatmap.

152 (f, g) Mice lungs were pre-educated with the indicated exosomes for 3 weeks,
153 and the CD11b and CD206 expression were analyzed by IHC. Representative
154 staining imaging (f) and relative H-score of CD11b and CD206 (g). n = 4
155 biologically independent mice. Data are mean \pm s.d. *P* values are shown.

156 (h) Mice were pre-educated with the indicated exosomes for 3 weeks, and
157 then were orthotopically injected with 143B-Luc cells. The lung metastases
158 were analyzed after 3 weeks. The lung metastases were analyzed by
159 bioluminescence. n = 5 biologically independent mice. Data are mean \pm s.d. *P*
160 values are shown.



161
162 **Figure. S7. The 1-10aa of RAB22A-NeoF1 is responsible for its binding to**
163 **PYK2.**

164 (a, b) 293T cells were co-transfected with the indicated plasmids and then
165 were lysed and analyzed by immunoprecipitation using anti-Flag beads (a) or

166 anti-V5 beads **(b)** followed by Western blotting.

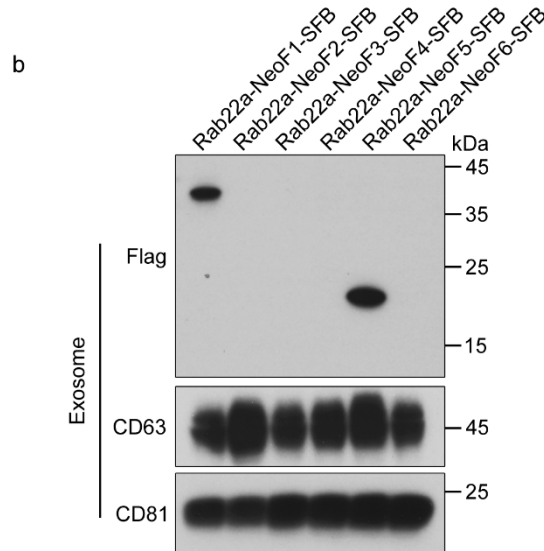
167 **(c, d)** 293T cells were co-transfected with the indicated plasmids and treated
168 with the indicated peptide for 24 h, and then were lysed and analyzed by
169 immunoprecipitation using anti-V5 beads **(c)** or anti-Flag beads **(d)** followed by
170 Western blotting. Data in a-d are representative of n = 3 biologically
171 independent experiments.

172 **(e)** U2OS cells were treated with the indicated exosomes for 24h, and then
173 were subjected to migration and invasion assays. Data are mean \pm s.d. of n = 3
174 biologically independent experiments. P values are shown.

175 **(f)** Bioluminescence analysis of lung metastatic foci from mice orthotopically
176 injected 143B-Luc cells with the indicated exosomes. n = 5 biologically
177 independent mice. Data are mean \pm s.d. P values are shown.

178 **(g)** Bioluminescence analysis of lung metastatic foci from mice orthotopically
179 co-injected U2OS/MTX300-Luc cells with ZOS-M cells at the 10:1 ratio under
180 the treatment of either 1-10aa-iRGD or random-iRGD peptide. n = 5
181 biologically independent mice. Data are mean \pm s.d. P values are shown.

a Rab22a-NeoF2: MALRELKVCLLGDTGVGKSSIVWRFVEDSFDPNINPTIGTVHNIKGTNPDAYQ
 Rab22a-NeoF3: MALRELKVCLLGDTGVGKSSIVWRFVEDSFDPNINPTIGFLILEGCCPSYLRG
 Rab22a-NeoF4: MALRELKVCLLGDTGVGKSSIVWRFVEDSFDPNINPTIGWSFTLVIPAGMQWHDLGSL
 QPPPPGFKQFACLSLLRSWNYRCSQPHLANFCSFSRDGVSPCWPGWSRTPDLR
 Rab22a-NeoF5: MALRELKVCLLGDTGVGKSSIVWRFVEDSFDPNINPTIGSRVQPCPWPF~~QLVVG~~DWFRYGHMT
 Rab22a-NeoF6: MALRELKVCLLGDTGVGKSSIVWRFVEDSFDPNINPTIGFKPIFPKDIQIGISI

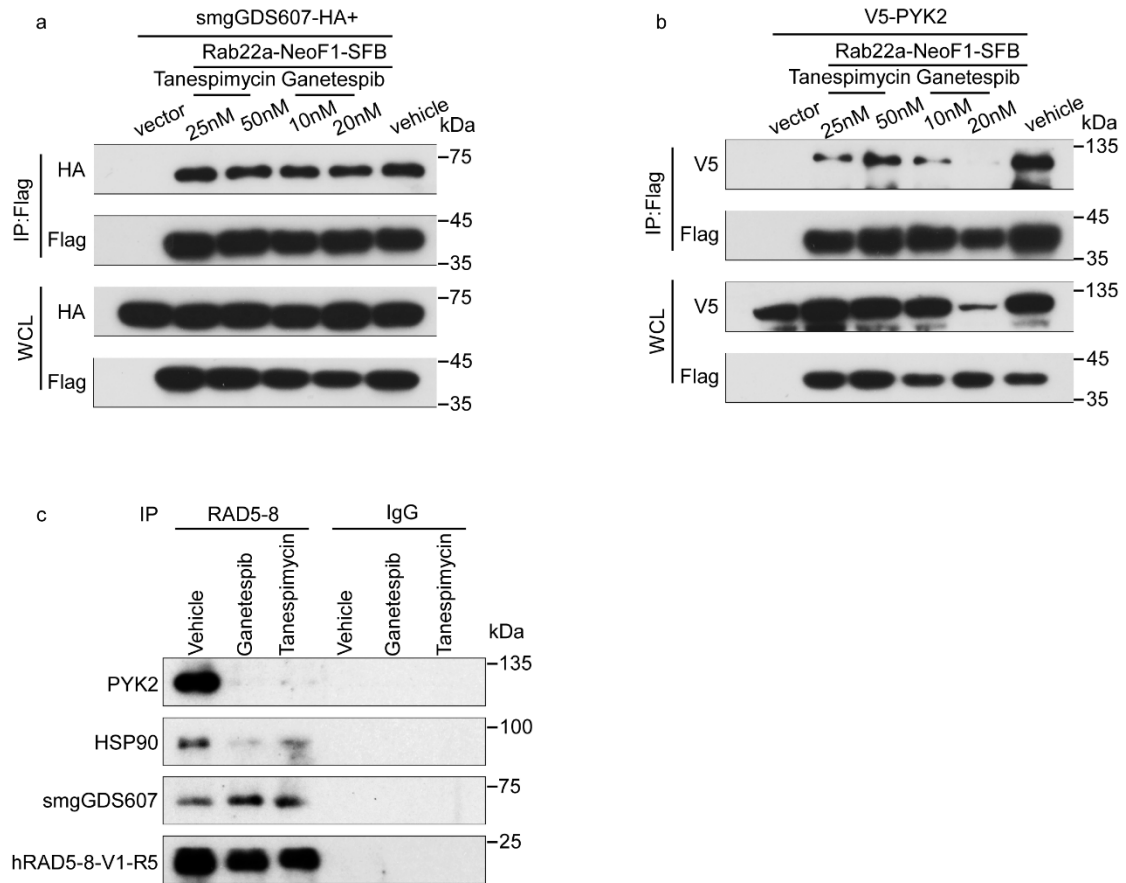


182

183 **Figure. S8. Secretion of RAB22A-NeoFs proteins**

184 (a) The protein sequences of RAB22A-NeoF2-6. The yellow region indicates
 185 the KFERQ-like motif (aa52-57).

186 (b) The exosomes derived from the indicated stable 143B cells were purified
 187 and subjected to Western blotting. Data are representative of n = 3 biologically
 188 independent experiments.



189

190 **Figure. S9. The interaction of RAB22A-NeoF1 fusion protein with PYK2,**
 191 **but not with smgGDS607, is dependent on its binding to HSP90.**

192 (a, b) 293T cells were co-transfected with the indicated plasmids and treated
 193 with the indicated HSP90 inhibitors for 24 h, and then were lysed and analyzed
 194 by immunoprecipitation using anti-Flag beads followed by Western blotting.

195 (c) ZOS-M cells were treated with the indicated HSP90 inhibitors for 24 h and
 196 then were lysed and subject to immunoprecipitation using IgG and mAb
 197 RAD5-8 followed by Western blotting. Data in a-c are representative of n = 3
 198 biologically independent experiments.